

**Delamination of open cylindrical shells from soft and adhesive Winkler's foundation**Oz Oshri <sup>\*</sup>*Department of Mechanical Engineering, Ben-Gurion University of the Negev, Beer-Sheva 84105, Israel*

(Received 25 May 2020; accepted 7 August 2020; published 8 September 2020)

The interaction between thin elastic films and soft-adhesive foundations has recently gained interest due to technological applications that require control over such objects. Motivated by these applications we investigate the equilibrium configuration of an open cylindrical shell with natural curvature  $\kappa$  and bending modulus  $B$  that is adhered to soft and adhesive foundation with stiffness  $K$ . We derive an analytical model that predicts the delamination criterion, i.e., the critical natural curvature,  $\kappa_{\text{cr}}$ , at which delamination first occurs, and the ultimate shape of the shell. While in the case of a rigid foundation,  $K \rightarrow \infty$ , our model recovers the known two-states solution at which the shell either remains completely attached to the substrate or completely detaches from it, on a soft foundation our model predicts the emergence of a new branch of solutions. This branch corresponds to partially adhered shells, where the contact zone between the shell and the substrate is finite and scales as  $\ell_w \sim (B/K)^{1/4}$ . In addition, we find that the criterion for delamination depends on the total length of the shell along the curved direction,  $L$ . While relatively short shells,  $L \sim \ell_w$ , transform continuously between adhered and delaminated solutions, long shells,  $L \gg \ell_w$ , transform discontinuously. Notably, our work provides insights into the detachment phenomena of thin elastic sheets from soft and adhesive foundations.

DOI: [10.1103/PhysRevE.102.033001](https://doi.org/10.1103/PhysRevE.102.033001)**I. INTRODUCTION**

Over the past few decades there has been renewed interest in the elasticity of slender bodies and their interaction with soft and adhesive foundations [1–23]. The motivation to study these systems comes from a wealth of technological applications that require control over the contact between such objects. For example, in the field of stretchable electronics and soft robotics [24], thin layers of electrical actuators are frequently placed on top of elastomeric robotic arms [25]. These arms are required to operate under extreme mechanical deformations while maintaining contact with the upper sensors. Any detachment between the two layers can potentially drive the deterioration of such devices. In contrast, some applications are motivated by the opposite functionality, which is to develop nondestructive methods for the removal of thin elastic layers from their adhesive surfaces. For example, many human diseases are initiated by the accumulation of plaque on the inner walls of arteries. This plaque corresponds to thin layer of bacteria that in the continuum limit can be viewed as a viscoelastic thin layer, or to leading order, as a thin elastic sheet. Recent studies developed a technique that utilizes wrinkles, which are regular undulations on the free surface of the thin film, to initiate detachment between the unwanted bacteria and the inner wall of an artery [26–29]. Furthermore, another motivation to study these adhesive interactions is related to geophysical systems [30,31], where glaciers are modeled as thin elastic beams that are resting on soft foundations with isolated regions of uplifting pressure. The criterion for the expansion of these isolated regions due to the underlying pressure, i.e., delamination, is usually obtained from the classical theory of fracture mechanics.

In the above examples the thin film was assumed flat in its rest configuration. However, in many cases these films accommodate nonzero curvatures even in their stress-free representation, i.e., they behave as shells rather than plates [32]. While in artificial materials shells emerge due to some predesign conditions, such as variations in the crosslink density along the thickness of a gel [33], in nature they emerge spontaneously due to irreversible processes that involve, for example, differential growth of internal fibers [34,35]. Despite the ubiquitous nature of these elastic structures, less attention was given in the literature to their interplay with an adhesive-compliant foundation and, moreover, to their effect on the detachment criterion. This criterion refers to the ultimate state of the system beyond which the shell detaches, either completely or partially, from the substrate. A numerical study that did consider this interaction was recently presented in Ref. [36], where a closed cylindrical shell was pulled from an adhesive foundation and revealed different regions in the force-displacement diagram. Another example, albeit without delamination, was presented in Refs. [37,38]. In this paper, elongated striplike shells with constant Gaussian curvature were placed on a fluid substrate. The interplay between the intrinsic curvature of the shell and its ability to stretch and bend in response to the hydrostatic pressure of the fluid resulted in rich morphological wrinkled structures.

In the present paper we aim to derive the detachment criterion at which a thin cylindrical shell with constant radius of curvature,  $\kappa^{-1}$ , and bending modulus,  $B$ , first delaminates from an adhesive substrate with stiffness  $K$ , and adhesion energy,  $w_{\text{ad}}$ . Hereafter we use the term “cylindrical shell” to denote thin elastic sheet with constant natural curvature,  $\kappa$ , that has two free edges. The analysis of this system in the case of a rigid substrate,  $K \rightarrow \infty$ , is well known ([39], p. 52) and relies on a boundary condition that prescribes

<sup>\*</sup>oshrioz@bgu.ac.il

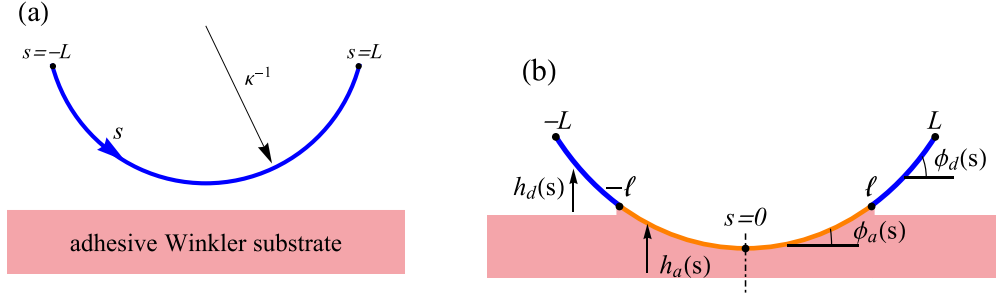


FIG. 1. Schematic overview of the system. (a) We consider a cylindrical shell that in the rest configuration has radius of curvature,  $\kappa^{-1}$ , and total length  $2L$ . Since the shell is inextensible the arclength parameter,  $s \in [-L, L]$ , remains unchanged between the undeformed and deformed configurations. Initially the shell is brought into contact with the adhesive substrate and then released to obtain the equilibrium configuration. (b) The final configuration can either remain completely adhered to the substrate,  $\ell = L$ , or partially adhered to the substrate,  $\ell < L$ . In either case, the profile is symmetric around  $s = 0$ . In the case of partial adhesion, the center of the shell remains adhered to the substrate (solid orange), and the tails (solid blue lines) are detached from the substrate. The deformed configuration is determined by four fields,  $h_a(s)$  and  $\phi_a(s)$  in the adhered region and  $h_d(s)$  and  $\phi_d(s)$  in the delaminated region.

discontinuous bending moments at the edges of the delaminated portion [16,40–44]. This analysis implies that below  $\kappa < \kappa_{\text{cr}} = \sqrt{2}/\ell_{\text{ec}}$ , where  $\ell_{\text{ec}} = (B/w_{\text{ad}})^{1/2}$  is the elastocapillary length scale [45], the shell remains completely adhered to the substrate, whereas above this critical value the shell completely detaches from the substrate. Evidently, this criterion neither depends on the total length of the shell, nor does it allow any partial contact with the substrate. Herein we show that when the assumption on the infinite rigidity of the substrate is relaxed, i.e.,  $K$  is finite, new branch of solutions emerges. The properties of these solutions deviate significantly from the observed behavior on a rigid substrate.

Our new solution relies on a previous work that considered the delamination of a uniaxially compressed sheet (not a shell) from soft and adhesive substrate [46]. In this formulation the interplay between the softness of the substrate and the adhesion energy was taken care of by a new boundary condition that allows continuous transition of momentum across the point of delamination. In particular, the new boundary condition accounted for the height of the sheet at the point of detachment, instead of the bending moment. In the respected limit of a rigid substrate the new, continuous, formulation converged into the known solution on a rigid substrate [16] up to narrow transition layers that are accommodated close to the take-off points.

Differently, when this new formulation is applied in the present cylindrical system it opens the door to a new branch of solutions that is qualitatively different from the solution on a rigid substrate. Within this new branch there are mechanically stable states with partial contact between the shell and the substrate. The length of the contact zone in these solutions scale as  $\ell \sim \ell_w$ , where  $\ell_w = (B/K)^{1/4}$  is the wrinkling length scale [9,17,47], and therefore diminishes to zero as  $K$  increases. In addition, we show that within the new branch the delamination criterion depends on the total length of shell,  $2L$ . When  $2L < 2\ell_* \simeq 5.54\ell_w$  the adhered-to-delaminated transition is continuous, i.e., of a second order, and is delayed compared to the corresponding criterion on a rigid substrate. However, when  $2L > 2\ell_*$  the adhered-to-delaminated transition is discontinuous, i.e., of a first order, and preempts the corresponding criterion on a rigid substrate.

The structure of the paper is as follows. In Sec. II we formulate the problem and derive the solution of this model in the case of a rigid substrate. In Sec. III we derive an approximated solution to shells that are partially adhered to the substrate and compare it with the numerical solution of the nonlinear equations. In Sec. IV we derive the delamination criterion. This section is divided into two parts. While in the first part we derive an approximated solution to shells that are completely adhered to the substrate, in the second part we analyze the transitions between adhered and delaminated solutions. Last, in Sec. V we conclude and summarize our main results.

## II. FORMULATION OF THE PROBLEM

We consider an inextensible cylindrical shell with radius of curvature  $\kappa^{-1}$ , bending modulus  $B$ , and total length  $2L$ , that is adhered to a soft substrate with stiffness  $K$  and adhesion energy  $w_{\text{ad}}$ , see Fig. 1(a). Given these physical constants, our goal is to develop a theoretical model that predicts the final configuration of the shell.

The deformation of the shell is described by two fields, one is the height function  $h(s)$  and second is the tangent angle  $\phi(s)$ , where  $s \in [-L, L]$  is the arclength along the center axis of the shell, see Fig. 1(b). The latter two fields are related by the geometric constraint,

$$\frac{dh}{ds} = \sin \phi. \quad (1)$$

The total energy of the system has two contributions. One from the adhered region,  $s < |\ell|$ , and second from the delaminated region,  $s > |\ell|$ ,

$$E[h(s), \phi(s)] = E_a[h_a(s), \phi_a(s)] + E_d[h_d(s), \phi_d(s)], \quad (2)$$

where in the forthcoming analysis we use the subscript and superscript “a” and “d” to denote quantities that are calculated in the adhered and the delaminated regions of the shell. In addition, we emphasize that the contact zone  $2\ell$  [see Fig. 1(b)] is *a priori* an unknown quantity; it will be determined from our analysis such as to minimize the total energy. While  $E_a$  accounts for (i) deviations from the natural curvature,  $\kappa$ , (ii)

the deformation of the substrate, and (iii) the adhesive interaction between the shell and the substrate, the delaminated energy,  $E_d$ , penalizes only bending deformations. Therefore, the energies in the corresponding regions are given by

$$E_a = 2 \int_0^\ell \left[ \frac{B}{2} \left( \frac{d\phi_a}{ds} - \kappa \right)^2 + \frac{K}{2} h_a^2 - w_{\text{ad}} \right] ds, \quad (3a)$$

$$E_d = 2 \int_\ell^L \left[ \frac{B}{2} \left( \frac{d\phi_d}{ds} - \kappa \right)^2 \right] ds. \quad (3b)$$

Since we anticipate the final solution to be symmetric around  $s = 0$ , we consider only one-half of the shell ( $s \geq 0$ ) and multiply the energy by a factor of 2. In addition, we assume a Winkler-type foundation that penalizes deviations from the stress-free configuration as in a series of linear harmonic springs [48,49]. We note that if the deformation of the substrate remains small compared with its flat, stress-free, configuration, then Winkler's energy becomes equivalent to that of a fluid foundation [8,46]. In the case of a fluid substrate the proportionality constant is given by  $K = \rho g$ , where  $\rho$  is the fluid density and  $g$  is the gravitational acceleration.

Overall, our system is defined using five independent constants,  $L$ ,  $\kappa$ ,  $B$ ,  $K$ , and  $w_{\text{ad}}$ , that yields four independent length scales. The total length  $2L$ , the radius of curvature  $\kappa^{-1}$ , the capillary length scale,  $\ell_c = (w_{\text{ad}}/K)^{1/2}$ , and the elasto-capillary length scale  $\ell_{\text{ec}} = (B/w_{\text{ad}})^{1/2}$ . Note that the latter two length scales yields the wrinkling length,  $\ell_w = (B/K)^{1/4}$ , that does not depend on  $w_{\text{ad}}$  but yet will play a role in our formulation.

To obtain the equilibrium configuration of the shell we need to minimize the total energy, Eqs. (2) and (3), given the geometric constraint, Eq. (1). To do that, we first normalize all lengths by  $\ell_w = (B/K)^{1/4}$  (i.e.,  $s \rightarrow s/\ell_w$ ) [50], the energy by  $B/\ell_w$ , and the adhesion by  $(BK)^{1/2}$ . Second, we follow the kinetic analogy in Ref. [7] and write  $\mathcal{S} = 2(\int_0^\ell \mathcal{L}_a ds + \int_\ell^L \mathcal{L}_d ds)$ , where

$$\mathcal{L}_a = \frac{1}{2} \left( \frac{d\phi_a}{ds} - \kappa \right)^2 + \frac{1}{2} h_a^2 - w_{\text{ad}} - p_h^a \left( \sin \phi_a - \frac{dh_a}{ds} \right), \quad (4a)$$

$$\mathcal{L}_d = \frac{1}{2} \left( \frac{d\phi_d}{ds} - \kappa \right)^2 - p_h^d \left( \sin \phi_d - \frac{dh_d}{ds} \right). \quad (4b)$$

In these equations  $p_h^a(s)$  and  $p_h^d(s)$  are Lagrange multipliers that enforce the geometric constraints in each region, Eq. (1) [51]. Physically these multipliers account for the total vertical force that the substrate exerts on the shell [46,52].

Third, we minimize Eq. (4) with respect to  $\phi_i$ ,  $h_i$ , and  $p_h^i$  ( $i = a, d$ ). This gives the following equilibrium equations in the adhered region:

$$\frac{d^2 \phi_a}{ds^2} + p_h^a \cos \phi_a = 0, \quad (5a)$$

$$\frac{dp_h^a}{ds} - h_a = 0, \quad (5b)$$

$$\frac{dh_a}{ds} - \sin \phi_a = 0, \quad (5c)$$

and in the delaminated region,

$$\frac{d^2 \phi_d}{ds^2} + p_h^d \cos \phi_d = 0, \quad (6a)$$

$$\frac{dp_h^d}{ds} = 0, \quad (6b)$$

$$\frac{dh_d}{ds} - \sin \phi_d = 0. \quad (6c)$$

Equations (5) and (6) form a closed system of equations once they are supplemented with nine boundary conditions; eight boundary conditions are necessary to solve Eqs. (5) and (6) and one to obtain the parameter  $\ell$ . The symmetry of the profile at  $s = 0$  gives

$$\phi_a(0) = 0, \quad (7a)$$

$$p_h^a(0) = 0. \quad (7b)$$

Continuity of the elastic shape and of momentum at  $s = \ell$  are taken care of by

$$h_a(\ell) = h_d(\ell), \quad (8a)$$

$$\phi_a(\ell) = \phi_d(\ell), \quad (8b)$$

$$\frac{d\phi_a}{ds}(\ell) = \frac{d\phi_d}{ds}(\ell), \quad (8c)$$

$$p_h^a(\ell) = p_h^d(\ell). \quad (8d)$$

Vanishing of forces and moments on the free edge of the delaminated section gives

$$p_h^d(L) = 0, \quad (9a)$$

$$\frac{d\phi_d}{ds}(L) = \kappa. \quad (9b)$$

Last, minimization of the total energy with respect to the parameter  $\ell$  yields the ninth boundary condition. This boundary condition is essentially equivalent to Griffith's theorem, which relates the interfacial toughness of the material to the energy release rate [16,40,41,53–55]. Following Appendix B in Ref. [46] we find the following condition:

$$h_a(\ell) = \sqrt{2w_{\text{ad}}}. \quad (10)$$

This completes the formulation of the problem. In summary, given the total length,  $2L$ , the natural curvature of the shell,  $\kappa$ , and the adhesion energy,  $w_{\text{ad}}$ , we can find the equilibrium configuration from the solution to Eqs. (5) and (6) and the boundary conditions Eqs. (7)–(10). In the following analysis we explore the energetical interplay between two possible solutions, one corresponding to shells that are completely adhered to the substrate ( $\ell = L$ ) and, second, to shells that are partially adhered to the substrate ( $\ell < L$ ). We will look for the critical natural curvature at which delamination becomes energetically favorable over the laminated solution. The total energy of a given shape is obtained from Eqs. (2) and (3).

#### A. The limit $K \rightarrow \infty$

We add a comment regarding the limit of a rigid substrate,  $K \rightarrow \infty$ . Retrieving dimensions into Eq. (10) gives  $h_a(\ell) = \sqrt{2}\ell_c$ , where  $\ell_c = (w_{\text{ad}}/K)^{1/2}$  is the capillary length

scale. Apparently, taking the limit  $K \rightarrow \infty$  leads to a singular formulation because  $h_a(\ell) \rightarrow 0$ , and the problem becomes independent on  $w_{ad}$  [56].

There are two routes to resolve this apparent singularity. The first route corresponds to our direction for obtaining the solution, i.e., no matter how stiff the substrate is, the height  $h_a(\ell)$  must always assume a finite value. The limit  $K \rightarrow \infty$  is thought only in the corresponding solution of the equilibrium equations. The second route corresponds to taking the limit  $K \rightarrow \infty$  in the elastic energy, even prior to minimization. This method is known to yield a discontinuous profile in the sense that the final configuration accommodates a discontinuity in the bending moments at the point of delamination [41].

Indeed, keeping in mind that on a rigid substrate  $d\phi_a/ds = 0$ , and in the free edge  $d\phi_a/ds = \kappa$ , we can immediately calculate the total energy of the shell from Eqs. (2) and (3). This gives  $E = 2\ell(\frac{1}{2}\kappa^2 - w_{ad})$ . Minimization of this energy with respect to  $\ell$ , i.e.,  $dE/d\ell = 0$ , gives the following delamination criterion:

$$\text{rigid substrate: } \kappa_{cr} = \sqrt{2w_{ad}}, \quad \Rightarrow \quad \kappa_{cr} = \sqrt{2}/\ell_{ec}, \quad (11)$$

where hereafter expressions given after an arrow correspond to the dimensional form of the preceding formula. When dimensions are retrieved into Eq. (11) we recover the familiar relation between the critical curvature and the elastocapillary length scale [16,39,41,57]. For a later comparison, note that Eq. (11) neither depends on the total length of the shell,  $2L$ , nor on the contact zone  $2\ell$ . Consequently, below the critical curvature,  $\kappa < \kappa_{cr}$ , the shell is completely adhered to the substrate, and above the critical curvature,  $\kappa > \kappa_{cr}$ , it is completely detached from the substrate.

Although the two routes converge in the limit  $K \rightarrow \infty$ , they deviate when  $K$  is assumed finite in the first route. As we shall see in the next section, this deviation is manifested both in the resulting shape of the shell and in the detachment criterion.

### III. APPROXIMATE SOLUTION TO PARTIALLY ADHERED SHELLS

In this section we seek an approximated solution to the problem under the assumption that  $w_{ad} \ll 1$ . This assumption has two consequences. First, using our normalization convention,  $w_{ad} = (\ell_c/\ell_w)^2$  and  $\ell_w = (\ell_c\ell_{ec})^{1/2}$ , it implies the scale separation,

$$\ell_c \ll \ell_w \ll \ell_{ec}. \quad (12)$$

Second, it allows us to linearize the equilibrium equations in the adhered region, i.e., using the approximation  $h_a(s) \ll 1$ . This is because the height at the point of delamination is proportional to the small parameter,  $h_a(\ell) \propto w_{ad}^{1/2} \sim \ell_c$  [see Eq. (10)]. Nonetheless, the delaminated region of the shell is in general not restricted to small deviations from the flat configuration, and therefore we keep its associated nonlinearities.

Solving Eq. (6) along with the linearized form of Eq. (5), i.e.,  $d^4h_a/ds^4 + h_a = 0$ , we obtain the following height

functions:

$$h_a(s) = \sqrt{2w_{ad}} \frac{[\cosh(2q\ell) - \cos(2q\ell)]^{1/2}}{\sin(2q\ell) - \sinh(2q\ell)} \times [e^{-qs} \cos(qs - \varphi_a) + e^{qs} \cos(qs + \varphi_a)], \quad (13a)$$

$$h_d(s) = (2w_{ad})^{1/2} + \frac{\cos(\kappa\ell + \varphi_d)}{\kappa} \left[ 1 - \frac{\cos(\kappa s + \varphi_d)}{\cos(\kappa\ell + \varphi_d)} \right], \quad (13b)$$

where  $q = 1/\sqrt{2}$  is the wave number of the profile in the adhered region and

$$\varphi_a = \tan^{-1} \left[ \frac{1 + \cot(q\ell) \tanh(q\ell)}{1 - \cot(q\ell) \tanh(q\ell)} \right],$$

$$\varphi_d = -\ell\kappa + 2q(2w_{ad})^{1/2} \frac{\cosh(2q\ell) - \cos(2q\ell)}{\sinh(2q\ell) - \sin(2q\ell)}, \quad (14)$$

are the phase shifts [58]. In the derivation of Eqs. (13) and (14) we used only eight out of the nine boundary conditions. To satisfy the ninth boundary condition this solution must be supplemented with the following equation that relates the natural curvature and the adhesion energy to the contact zone:

$$\frac{\sinh(2q\ell) + \sin(2q\ell)}{\sinh(2q\ell) - \sin(2q\ell)} = \frac{\kappa}{(2w_{ad})^{1/2}}. \quad (15)$$

Given  $\kappa$  and  $w_{ad}$  we can now solve Eq. (15) to obtain  $\ell$ . Following the graphical solution of this equation in Fig. 2(a), we find that up to  $\kappa/(2w_{ad})^{1/2} \lesssim 0.94$  no solution exists. At  $\kappa_*/(2w_{ad})^{1/2} \simeq 0.94$  a delaminated solution with  $\ell_* \simeq 2.77$  first becomes available [59]. When  $0.94 \lesssim \kappa/(2w_{ad})^{1/2} \lesssim 1$  there are two possible solutions, one with decreasing values of  $\ell$  and second with increasing  $\ell$ , see the inset of Fig. 2(a). As can be verified by direct substitution in the total energy, Eq. (2), the former solution, with smaller values of  $\ell$ , is always energetically favorable over the latter one. We note that this subtlety of multiple solutions is similar in nature to observations made in other adhesion related systems [43,46,60]. Last, when  $\kappa/(2w_{ad})^{1/2} \gtrsim 1$  the solution for  $\ell$  is unique. In the latter region, when the solution is unique, some analytical approximation of Eq. (15) can be derived. Expanding the left-hand side of Eq. (15) in powers of  $\ell$  gives to leading order,

$$\frac{3}{\ell^2} \simeq \frac{\kappa}{(2w_{ad})^{1/2}}. \quad (16)$$

This approximation is plotted in Fig. 2(a) (black dashed line) along with the exact function (blue solid line). The two lines deviate at large values of  $\ell$  but tend to coincide starting from  $\ell \lesssim 1.0$ .

We emphasize that even if a delaminated solution becomes available, it yet may not be the global minimizer of the problem. The experimentally observed pattern is selected among all possible solutions, adhered and delaminated, such as to minimize the total energy. Further discussions on these adhered-to-delaminated transitions are kept to the next section.

This completes the approximated solution. In summary, given the natural curvature of the shell,  $\kappa$ , and the adhesion energy,  $w_{ad}$ , we first obtain  $\ell$  from Eq. (15) and then determine the height profile from Eqs. (13) and (14). In Fig. 2(b) we

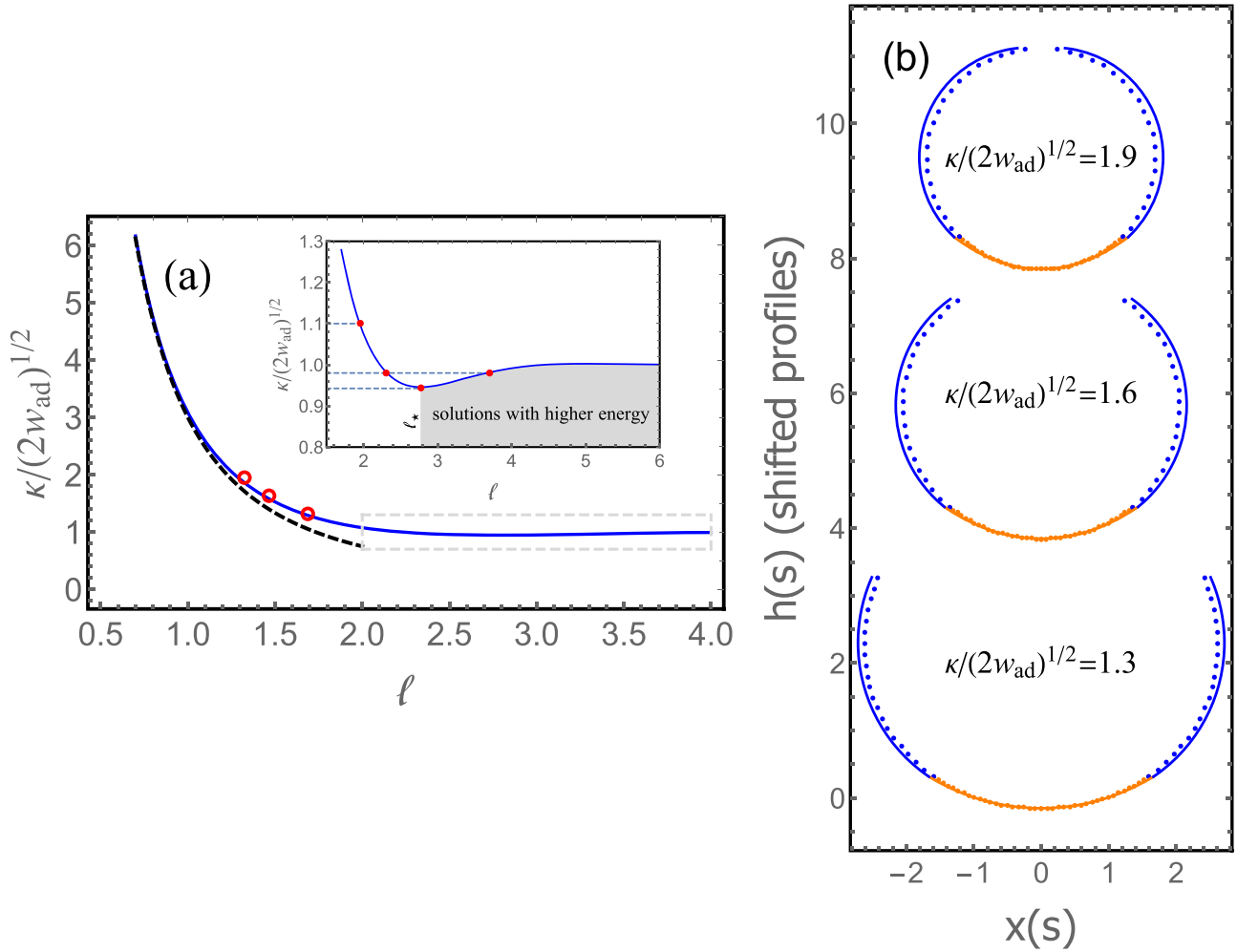


FIG. 2. Solutions to Eq. (15) and plots of the shell’s configuration. (a) Graphical solution of Eq. (15). The parameter  $\kappa/(2w_{ad})^{1/2}$  is plotted as a function of the normalized adhered length,  $\ell$ . While the solid blue line represents the function on the left-hand side of Eq. (15), the black dashed line represents the approximated solution at small  $\ell$ , which is  $\kappa/(2w_{ad})^{1/2} \simeq 3/\ell^2$ , see Eq. (16). The open red circles represents the numerical solution of the nonlinear equations at  $\kappa/(2w_{ad})^{1/2}$  that are considered in panel (b). Inset: Zoom-in the area indicated by the dashed light gray rectangle. Up to  $\kappa_*/(2w_{ad})^{1/2} \simeq 0.94$  there is no solution to Eq. (15). At this critical value partial adhered solution with  $\ell_* \simeq 2.77$  first becomes available. Above it,  $0.94 \lesssim \kappa/(2w_{ad})^{1/2} \lesssim 1$ , there are two possible solutions, one with  $\ell \lesssim 2.77$  and second with  $\ell \gtrsim 2.77$ ; the former solutions are energetically favorable over the latter ones. Beyond  $\kappa/(2w_{ad})^{1/2} \gtrsim 1$  the solution is always unique. (b) The profile of the shell is plotted for several values of the parameter  $\kappa/(2w_{ad})^{1/2}$  where  $2L = 10$  and  $w_{ad} = 0.05$ . The analytical solution (solid lines) is compared with the numerical solution (dots) of Eqs. (5) and (6). In both cases orange and blue colors correspond to adhered and delaminated regions, respectively. For clarity, the different profiles of the shell are shifted along the  $y$  direction. Keeping in mind the even parity of the solution, the analytical profile in the adhered region,  $(s, h_a(s))$ , is given by Eqs. (13a) and (14), where  $\ell$  is determined from Eq. (15). The delaminated profile  $(x_d(s), h_d(s))$  is given by Eqs. (13b) and (14), where  $x_d(s) = \ell + \int_{\ell}^s \cos \phi_d(s') ds'$ .

plot this solution for a given  $w_{ad}$  and for several values of  $\kappa$ , and compare the results with the numerical solution of the complete set of nonlinear equations. The relatively good fit between the two solutions, approximated and numerically exact, essentially validates our set of simplifying assumptions.

We add several comments regarding this solution. First, although the total length of the shell,  $2L$ , appears in our boundary conditions, Eq. (9), it does not play a role in Eqs. (13)–(15). This is because the delaminated part of the shell is free, and therefore an extension of the total length by some increment does not change the energy of the body. One may then ask the following question: What happens if  $L < \ell$ , where  $\ell$  is the solution of Eq. (15)? In that case our de-

laminated solution does not even exist because the boundary condition at the shell’s edge, Eq. (9b), is not properly satisfied. Consequently, although  $L$  does not explicitly appear in this solution, it does have an effect on the resulting morphology in some range of the parameter space.

Second, retrieving dimensions into the right-hand side of Eq. (15) we find that  $\kappa/\sqrt{2w_{ad}} \rightarrow \kappa/(\sqrt{2}/\ell_{ec})$ , where  $\ell_{ec} = (B/w_{ad})^{1/2}$  is the elastocapillary length scale. Indeed, although our formulation does not involve this length scale explicitly, it appears naturally in the boundary conditions. We note that scaling argument for the geometrical interplay among  $\ell_c$ ,  $\ell_w$ , and  $\kappa$  that gives rise to  $\ell_{ec}$  was given in Ref. [45] regarding another adhesion related system.

Third, the total elastic energy of this partially adhered solution is obtained from Eq. (3a), i.e., the adhered region. Obviously, the energy of the free, delaminated, region, Eq. (3b), vanishes [61]. Substituting Eqs. (13a) and (14) in Eq. (3a) and integrating gives

$$\begin{aligned} & E(\kappa/(2w_{\text{ad}})^{1/2}, \ell)/w_{\text{ad}} \\ &= 2\ell \left\{ \left[ \frac{\kappa}{(2w_{\text{ad}})^{1/2}} \right]^2 - 1 \right\} - 2^{3/2} \left[ 1 + 2 \frac{\kappa}{(2w_{\text{ad}})^{1/2}} \right] \\ & \quad \times \frac{\cosh(\sqrt{2}\ell) - \cos(\sqrt{2}\ell)}{\sinh(\sqrt{2}\ell) - \sin(\sqrt{2}\ell)} \\ & \quad + \frac{4\sqrt{2}[\cosh(\sqrt{2}\ell) - \cos(\sqrt{2}\ell)] \sinh(\sqrt{2}\ell)}{[\sinh(\sqrt{2}\ell) - \sin(\sqrt{2}\ell)]^2}, \quad (17) \end{aligned}$$

where we substituted  $q = 1/\sqrt{2}$  in order to simplify the final expression, and we keep in mind that  $\ell$  is determined from Eq. (15). Note that Eq. (17) essentially depends on the parameter  $\kappa/(2w_{\text{ad}})^{1/2}$  and not on  $\kappa$  alone.

Last, comparing this solution with the solution of a rigid substrate, Sec. II A, we can already point to the first and important deviation between them. When the assumption on the substrate's stiffness is relaxed new branch of solutions emerges. This branch corresponds to partially adhered shells where the contact zone,  $\ell/\ell_w$  (in dimensional form), remains finite. Within this solution, the limit of a rigid substrate is recovered when  $\ell_w = (B/K)^{1/4} \rightarrow 0$ .

#### IV. TRANSITIONS BETWEEN ADHERED AND DELAMINATED SOLUTIONS ON SOFT SUBSTRATE

In this section we derive the adhered-to-delamination criterion. For a given strength of the adhesion energy,  $w_{\text{ad}}$ , we are interested in obtaining the critical curvature,  $\kappa_{\text{cr}}$ , at which delamination first occurs. To do that, we divide the section into two parts. In the first part we derive the solution of a shell that is completely adhered to the substrate and calculate its total energy, and in the second part, we compare the energies of the two solutions, delaminated and adhered, and derive the delamination criterion.

##### A. Solution to completely adhered shells

In this section we aim to find the energy of shells that are completely adhered to the substrate. Since adhesion no longer affects the final configuration, we anticipate this solution to depend only on three, out of the four, independent length scales,  $\ell_w = (B/K)^{1/4}$ ,  $L$  and  $\kappa^{-1}$ .

In the previous section we showed that delaminated solutions become available when  $\kappa/(2w_{\text{ad}}) \sim 1$ . Since we anticipate an adhered-to-delaminated transition around this value, and  $w_{\text{ad}}$  was assumed small, we will restrict ourselves in this section to cases where  $\kappa \ll 1$ . To obtain the height function of the shell under this approximation, we linearize Eq. (5) and solve them together with four boundary conditions; two at  $s = 0$ , Eq. (7), and two at the free edge, Eq. (9). To differentiate between this completely adhered solution, and the previous,

partially adhered solution, we will use the subscript 'ca' on the corresponding quantities. The solution reads [62]

$$\begin{aligned} h_{\text{ca}}(s) &= \frac{\kappa [\cosh(2qL) - \cos(2qL)]^{1/2}}{2q^2 [\sinh(2qL) + \sin(2qL)]} \\ & \quad \times [e^{-qs} \cos(qs - \varphi_{\text{ca}}) + e^{qs} \cos(qs + \varphi_{\text{ca}})], \quad (18a) \end{aligned}$$

$$\varphi_{\text{ca}} = \tan^{-1} \left[ \frac{1 + \cot(qL) \tanh(qL)}{1 - \cot(qL) \tanh(qL)} \right], \quad (18b)$$

where  $q = 1/\sqrt{2}$ . Indeed, in this linearized solution the height profile is proportional to  $\kappa$ , which is our small parameter. In Figs. 3(a) and 3(b) we plot this height profile for several values of  $L$ , and compare it with the solution of the nonlinear equations, Eq. (5).

Examining the resulting shapes we identify two distinct limits within this linearized solution. When the total length of the shell is smaller than the characteristic decay length, i.e.,  $qL \ll 1$ , the configuration remains approximately circular. This configuration is extensive in the sense that its maximum amplitude scales with  $L$ . When the shell is very long,  $qL \gg 1$ , the deformation becomes localized around  $s = L$  at a narrow region of length  $\sim 1/q$ . In both limits the approximated form of Eq. (18) and their corresponding energies, Eq. (3a), are given by

$$qL \ll 1: h_{\text{ca}}(s) = \frac{\kappa L^2}{6} \left( \frac{3s^2}{L^2} - 1 \right), E_{\text{ca}} - E_o \simeq \frac{L^5 \kappa^2}{45}, \quad (19a)$$

$$\begin{aligned} qL \gg 1: h_{\text{ca}}(s) &= \frac{\kappa}{2q^2} e^{-q\zeta} [\cos(q\zeta) - \sin(q\zeta)], \\ E_{\text{ca}} - E_o &\simeq L\kappa^2, \quad (19b) \end{aligned}$$

where  $\zeta = L - s$  measures the relative distance from the edge,  $E_o = -2Lw_{\text{ad}}$  is the adhesion energy, and to derive the solution in Eq. (19b) we neglected the boundary conditions at  $s = 0$ , Eq. (7). In addition, to derive the energy in Eq. (19b) we kept terms of order  $\kappa L$  in tact, but neglected terms of order  $e^{-qL}$  and  $\kappa^2$ . These approximations are plotted in Fig. 3 (dashed black lines) along with the linearized (solid orange) and exact numerical solutions (dots). While Fig. 3(a) corresponds to relatively short shells, where Eq. (19a) holds, Fig. 3(b) correspond to long shells, where Eq. (19b) holds. At approximately  $L \simeq 2.5$  we find a transition between the two limiting solutions. Indeed, comparing the energies of the two approximations, Eqs. (19a) and (19b), gives the critical length,  $L \simeq 2.59$ . In addition, in Fig. 3(c) we plot the maximum height of the profile,  $h_{\text{ca}}(L)$ . When  $L \ll 1$  the maximum height growth parabolically as  $h_{\text{ca}} = \kappa L^2/3$ , see Eq. (19a), and when  $L \gg 1$  it saturates and approaches an ultimate value of  $h_{\text{ca}}(L) = \kappa/(2q^2)$ , see Eq. (19b).

As is further discussed in the next section, this transition between extensive and localized shapes affects the adhered-to-delamination transition. While relatively short shells transform continuously into a delaminated state, long shells present discontinuous jump.

Last, we calculate the energy of the linearized profile. Substituting Eq. (18) in the total elastic energy of the adhered

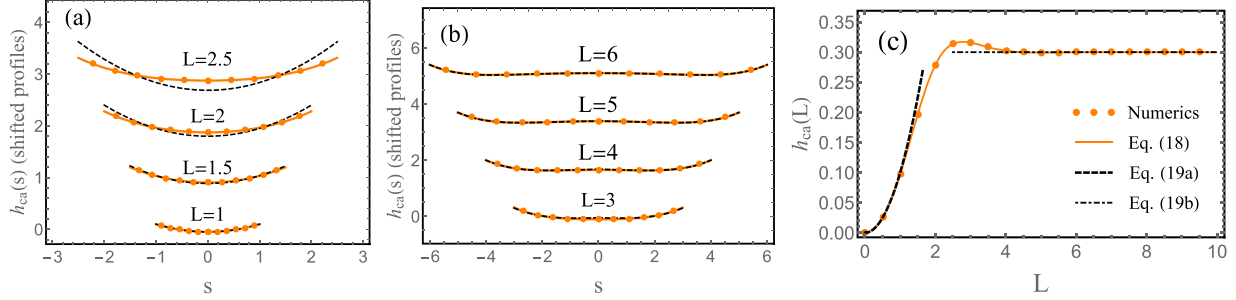


FIG. 3. The height profiles of completely adhered shells ( $\kappa = 0.3$ ). In panels (a) and (b) solid-orange lines correspond to the solution of the linear equations, Eq. (18), dots to the numerical solution of the nonlinear equations, Eq. (5), and dashed black lines to the approximations, Eq. (19). For clarity, the profiles are shifted along the  $y$  direction. While relatively short shells are plotted in panel (a) and are approximated by Eq. (19a), long shells are plotted in panel (b) and are approximated by Eq. (19b). The circular approximation to the elastic profile breaks down at  $L \simeq 2.5$ . (c) The maximum height of the shell as a function of the total length. When  $L$  is small the height is proportional to  $h_{ca}(L) = \kappa L^2/3$  [see Eq. (19a)], and when  $L$  is large the maximum height saturates and equals  $h_{ca}(L) = \kappa/(2q^2)$  [see Eq. (19b)]. As in previous panels, dots corresponds to the numerical solution of Eq. (5) and solid orange line to Eq. (18).

region, Eq. (3a), and integrating gives,

$$\begin{aligned} & E_{ca}(\kappa/(2w_{ad})^{1/2}, L)/w_{ad} \\ &= 2L \left\{ \left[ \frac{\kappa}{(2w_{ad})^{1/2}} \right]^2 - 1 \right\} \\ &+ 2^{3/2} \left[ \frac{\kappa}{(2w_{ad})^{1/2}} \right]^2 \frac{\cos(\sqrt{2}L) - \cosh(\sqrt{2}L)}{\sin(\sqrt{2}L) + \sinh(\sqrt{2}L)}, \quad (20) \end{aligned}$$

where in order to simplify the final expression we substituted  $q = 1/\sqrt{2}$ . Equation (20) reduces to the expressions given in Eq. (19) in their respective limits of approximations. Note that similarly to Eq. (17) this energy depends on the parameter  $\kappa/(2w_{ad})^{1/2}$ , and not on  $\kappa$  alone. Note also that the solution derived in this section is limited by the assumption that  $\kappa \ll 1$ , i.e., the natural radius of curvature of the shell must be much larger than the characteristic wrinkling length scale. This restriction is equivalent to the requirement that the amplitude of the resulting elastic shape remains small.

## B. Adhered-to-delamination criterion

In this section we drive the delamination criterion, i.e., given  $w_{ad}$  and  $L$  we look for the critical curvature,  $\kappa_{cr}$ , and the critical contact zone,  $\ell_{cr}$ , at the adhered-to-delamination transition. In accordance with the standard terminology of critical phenomena,  $\kappa$  and  $m \equiv (L - \ell)^{1/2}$  will be referred to as the control and order parameters of the transition respectively.

This section is divided into two parts. In the first part we present the evolution of the energy landscape,  $\Delta E = E - E_{ca}$ , as a function of the control parameter  $\kappa$ , and highlight two different regions in its behavior with respect to the total length of the sheet. In the second part, we derive an approximated quantitative criterion for the delamination in each region.

### 1. Qualitative analysis of the energy landscape

As a first step in the analysis we focus on the evolution of the energy landscape. Following Ref. [63] we calculate the energy difference,

$$\Delta E = E(\kappa/(2w_{ad})^{1/2}, \ell) - E_{ca}(\kappa/(2w_{ad})^{1/2}, L), \quad (21)$$

where  $E(\kappa/(2w_{ad})^{1/2}, \ell)$  and  $E_{ca}(\kappa/(2w_{ad})^{1/2}, L)$  are given by Eqs. (17) and (20) respectively. Two examples for the typical evolution of  $\Delta E$  as a function of  $\kappa/(2w_{ad})$  and  $\ell$ , where  $L = 6$  and  $L = 2$ , are plotted in Fig. 4. These examples suggests that the adhered-to-delamination transition behaves differently depending on whether  $L > \ell_*$  or  $L < \ell_*$ . We remind the reader that  $\ell_* \simeq 2.77$  corresponds to the contact zone at which delaminated solution first becomes available, see Fig. 2(a).

On one hand, if  $L > \ell_*$  [Fig. 4(a)] the energy landscape exhibits a first order transition. Namely, when  $\kappa/(2w_{ad})^{1/2} \lesssim 0.94$ , the global minimizer is always  $\ell = L$ . At  $\kappa/(2w_{ad})^{1/2} \simeq 0.94$  an inflection point (spinodal) appears in  $\Delta E$ , but yet the global minimizer is unchanged. When  $\kappa/(2w_{ad})^{1/2} \gtrsim 0.94$  new local minima appears. This minima becomes the global minimizer when  $\kappa/(2w_{ad})^{1/2} \gtrsim 1$ . On the other hand, if  $L < \ell_*$  [Fig. 4(b)], then the energy landscape exhibits a second order transition. The global minima is  $\ell = L$  until  $\kappa/(2w_{ad})$  is crossing a certain threshold. Beyond this threshold,  $\ell$  is continuously decreasing to zero.

The different behavior of the transition as a function of  $L$  can be explained from the graphical solution of Eq. (15), see Fig. 2(a). Indeed, one can verify that minimization of the energy landscape, Eq. (21), with respect to  $\ell$  gives this equation. If  $L > \ell_*$ , then the inflection point in  $\Delta E$  corresponds to the critical confinement  $\kappa/(2w_{ad})^{1/2} \simeq 0.94$  at which the delaminated solution becomes available. The system then jumps into this new solution, as in a first order transition, when it overcomes some energetical barrier [64], or when the control parameter is made large enough. Contrary, when  $L < \ell_*$  the delaminated solution does not even exist if the solution of Eq. (15), i.e.,  $\ell$ , is greater than total length,  $L$ . In that case, the transition is delayed until  $\kappa/(2w_{ad})^{1/2}$  is made large enough so as the solution of Eq. (15) satisfies  $\ell = L$ . Beyond this critical point, delamination progresses continuously according to the solutions of Eq. (15).

### 2. Approximated quantitative criteria for delamination

As a second step in the analysis we are interested to derive quantitative criteria for delamination. For this reason, we will

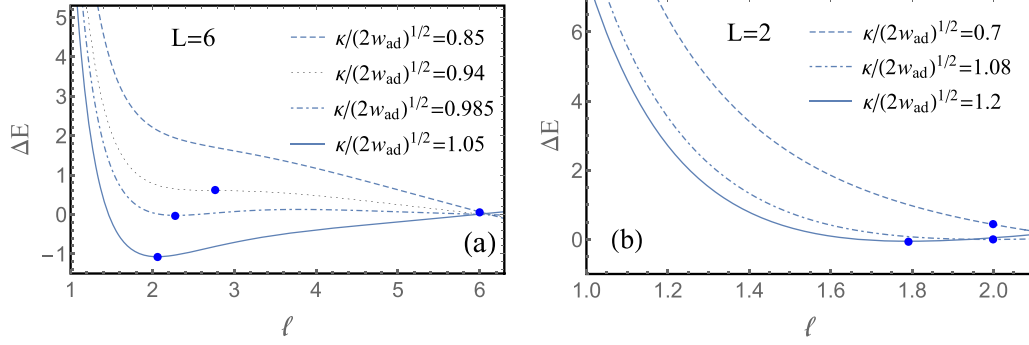


FIG. 4. Examples of the energy landscape for two different total lengths, (a)  $L = 6 > \ell_*$  and (b)  $L = 2 < \ell_*$ . In both panels the energy difference, Eq. (21), is plotted as a function of the adhered length,  $\ell$ , for several values of  $\kappa/(2w_{\text{ad}})^{1/2}$ . The blue dots on each curve indicate the local minima. While the behavior depicted in panel (a) corresponds to a discontinuous, first order transition, the behavior in panel (b) corresponds to a continuous, second order transition.

assume that at the transition the energies of the two solutions, adhered and partially adhered, coincide. Of course, if the transition is of a first order, then the system yet needs to cross some energetical barrier to jump into the new equilibrium state. Keeping in mind that the contact zone is determined from Eq. (15), we obtain a system of two equations for the two unknowns  $\kappa_{\text{cr}}$  and  $\ell_{\text{cr}}$ ,

$$\Delta E: E\left(\frac{\kappa_{\text{cr}}}{(2w_{\text{ad}})^{1/2}}, \ell_{\text{cr}}\right) = E_{\text{ca}}\left(\frac{\kappa_{\text{cr}}}{(2w_{\text{ad}})^{1/2}}, L\right), \quad (22a)$$

$$\frac{\kappa_{\text{cr}}}{(2w_{\text{ad}})^{1/2}} = \frac{\sinh(2q\ell_{\text{cr}}) + \sin(2q\ell_{\text{cr}})}{\sinh(2q\ell_{\text{cr}}) - \sin(2q\ell_{\text{cr}})}, \quad (22b)$$

Since both energies depend on the parameter  $\kappa/(2w_{\text{ad}})^{1/2}$  we can just substitute the right-hand side of Eq. (22b) in Eq. (22a), and obtain an equation for  $\ell_{\text{cr}}$ ,

$$E(\ell_{\text{cr}}) - E_{\text{ca}}(\ell_{\text{cr}}, L) = 0, \quad (23)$$

where  $L$  is a free parameter. In Fig. 5(a) we plot the solutions of this equation as a function of  $L$ .

When  $L < \ell_*$  we find that Eq. (23) has the unique solution  $\ell_{\text{cr}} = L$ . Substituting this solution in Eq. (22b) gives the critical curvature at the onset of the instability,

soft substrate ( $L < \ell_*$ ):

$$\begin{aligned} \kappa_{\text{cr}} &= (2w_{\text{ad}})^{1/2} \frac{\sinh(2qL) + \sin(2qL)}{\sinh(2qL) - \sin(2qL)} \simeq 3 \frac{(2w_{\text{ad}})^{1/2}}{L^2}, \\ \Rightarrow \kappa_{\text{cr}} &\simeq 3\sqrt{2} \frac{\ell_c}{L^2}, \end{aligned} \quad (24)$$

where the last equality is the leading order expansion in power of  $L$  [65].

After the initial detachment the adhered length  $\ell$  is determined from Eq. (15), or by its approximated form, Eq. (16). Note that within the latter approximation the order parameter at the vicinity of the instability is given by,

$$m \simeq (3/4)^{1/4} \left[ \frac{(2w_{\text{ad}})^{1/2}}{\kappa_{\text{cr}}} \right]^{1/4} [(\kappa - \kappa_{\text{cr}})/\kappa_{\text{cr}}]^{1/2}, \quad (25)$$

with a critical exponent of  $\beta = 1/2$ , that is expected from a continuous, second order transition. In Fig. 5(b) we plot the detachment criterion, Eq. (24), in comparison with Eq. (11),

that corresponds to the criterion on a rigid substrate. Evidently, in this region of the parameter space delamination is delayed compared to the expected behavior on a rigid substrate. In other words, decreasing the stiffness of the substrate,  $K$ , or the total length,  $L$ , increase the critical curvature  $\kappa_{\text{cr}}$  at which delamination occurs.

When  $L > \ell_*$  new branch emerges in the solution of Eq. (23), see Fig. 5(a). Notably, the new branch quickly converges to a constant  $\ell_{\text{cr}} = \pi/\sqrt{2} < \ell_*$ , which is independent on  $L$ . Since solutions with  $\ell > \ell_*$  are always higher in energy compared to solutions with  $\ell < \ell_*$  [see Fig. 2(a)], the new branch is energetically preferable over the previous one,  $\ell_{\text{cr}} = L$ . We note that other branches bifurcate from the unstable branch,  $\ell_{\text{cr}} = L$ , beyond  $L > \ell_*$ , however, they are not shown in Fig. 5(a). These branches correspond to solutions with  $\ell > \ell_*$ , and therefore are unstable.

To approximate the critical curvature and contact zone in the new branch we employ the long shells approximation and expand  $\kappa_{\text{cr}}$  and  $\ell_{\text{cr}}$  in powers of  $1/L$ . Solving Eq. (22) perturbatively within this expansion gives,

soft substrate ( $L > \ell_*$ ):

$$\begin{aligned} \kappa_{\text{cr}} &\simeq (2w_{\text{ad}})^{1/2} \left(1 + \frac{a_1}{L}\right), \\ \Rightarrow \kappa_{\text{cr}} &\simeq \frac{\sqrt{2}}{\ell_{\text{ec}}} \left(1 + a_1 \frac{\ell_w}{L}\right), \end{aligned} \quad (26a)$$

$$\begin{aligned} \ell_{\text{cr}} &\simeq \frac{\pi}{\sqrt{2}} + \frac{b_1}{L}, \\ \Rightarrow \ell_{\text{cr}} &\simeq \left(\frac{\pi}{\sqrt{2}} + b_1 \frac{\ell_w}{L}\right) \ell_w, \end{aligned} \quad (26b)$$

where  $a_1 = (1 - \coth \pi - 1/\sinh \pi)/\sqrt{2}$  and  $b_1 = (1 + \cosh \pi - \sinh \pi)/4$  are negative and positive constants respectively. Equation (26b) is plotted in Fig. 5(a) along with the exact solution of Eq. (23). While the two solutions, approximated and exact, deviate close to  $L = \ell_*$ , they tend to coincide when  $L \gtrsim 4$ . Obviously, this branch of solutions corresponds to a discontinuous transition. When detachment occurs, the order parameter jumps from zero to a finite value,  $m \simeq (L - \pi/\sqrt{2})^{1/2}$ , as in a first order transition.

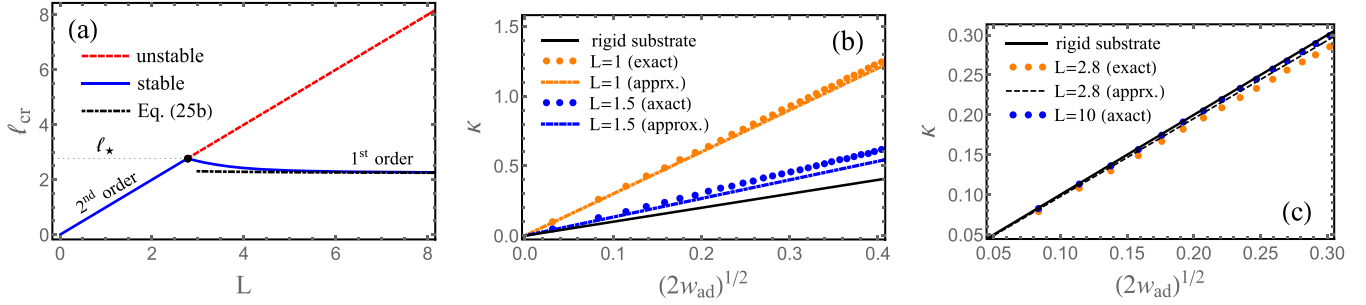


FIG. 5. Critical contact zone,  $l_{cr}$ , and state diagrams of the adhered-to-delamination transition. (a) Solutions of Eq. (23) as a function of  $L$ . Up to  $l_{cr} < l_*$  the solution is unique and is given by  $l_{cr} = L$  (solid blue line). At  $l_{cr} = l_*$  (black dot) the solution bifurcates into two branches. One corresponding to  $l_{cr} = L$  (dashed red line), and a new branch that converges to the constant  $l_{cr}(L \gg 1) \simeq \pi/\sqrt{2}$  (solid blue line). When the long shell approximation is invoked for the latter branch, its asymptotic behavior is given by Eq. (26b) (dashed dotted black line). Since the first branch corresponds to solutions with  $l > l_*$ , and the second to  $l < l_*$ , the latter set of solutions is always energetically preferable over the first one. While stable solutions with  $L < l_*$  transform continuously, as in a second order transition, into a delaminated state, stable solutions with  $L > l_*$  transform discontinuously, as in a first order transition. (b) State diagram of short shells ( $L < l_*$ ). The curvature,  $\kappa$ , is plotted as a function of the adhesion parameter,  $(2w_{ad})^{1/2}$ , for several values of  $L$ . While blue and orange dots represents the critical lines at which delamination occurs, i.e., the numerical solution of Eq. (22), the corresponding dashed lines represents the approximation that is given by Eq. (24). The solid black line corresponds to the delamination criterion of a rigid substrate, Eq. (11). For a given  $w_{ad}$ , the critical curvature increases as the total length decreases. (c) State diagram of long shells ( $L > l_*$ ), where the axes are as in panel (b). While orange and blue dots corresponds to the numerical solution of Eq. (22) at different total lengths, dashed black line corresponds to the long shells approximation, Eq. (26a). Solid black line is the rigid criterion, Eq. (11). As the total length increases the criteria on soft and rigid substrates tend to coincide. Nonetheless, for any finite  $L$  and at a given  $w_{ad}$  the delamination criterion on soft substrate slightly preempt the expected criterion on a rigid substrate.

In Fig. 5(c) we plot the delamination criterion, Eq. (26a) and compare the results with Eq. (11) for a rigid substrate. In different from short shells, Eq. (24), now delamination slightly preempts the rigid criterion. However, as the total length increases the two criteria, on soft and rigid substrates, tend to coincide. Indeed, in the limit of a rigid substrate we have that,  $l_w = (B/K)^{1/4} \rightarrow 0$ , and therefore  $\kappa_{cr} \rightarrow \sqrt{2}/l_{ec}$  and  $l_{cr} \rightarrow 0$ , as predicted by Eq. (11).

This completes the adhered-to-delamination analysis. In summary, given the adhesion energy and the total length,  $w_{ad}$  and  $2L$ , we obtain the critical curvature and the contact zone,  $\kappa_{cr}$  and  $l_{cr}$ , from the solution of Eqs. (22). The solution of these equations can be divided into two main branches. One corresponding to short shells ( $L < l_*$ ), that undergo continuous transition where  $l_{cr} = L$  and  $\kappa_{cr}$  is given in Eq. (24), and second corresponding to long shells ( $L > l_*$ ), that undergo discontinuous transition where  $l_{cr}$  and  $\kappa_{cr}$  are approximated in Eq. (26). While in the first branch delamination is delayed compared to the criterion of a rigid substrate, Eq. (11), in the second branch delamination preempt the rigid criterion. In the limit of a rigid substrate the bifurcation point [black dot in Fig. 5(a)] is shifted toward the origin, such that the first branch of solutions no longer exists and  $l_{cr} \rightarrow 0$  for all values of  $L$ .

## V. CONCLUSIONS

In this manuscript we analyzed the delamination of a thin cylindrical shell from a soft and adhesive foundation. Following the analysis in Ref. [46] we derived a set of nonlinear equilibrium equations, Eqs. (5)–(10), that predict the final configuration of the shell as a function of the system parameters,  $L$ ,  $\kappa$ ,  $B$ ,  $K$ , and  $w_{ad}$ . Notably, this formulation guarantees continuous transfer of linear and angular momentum across the point of delamination,  $l$ , and therefore provides

more realistic description of the detachment phenomena. In different from the expected behavior on a rigid substrate, we showed that the solution of these equations corresponds to partially adhered shells that have finite contact zone.

An analytical approximation to these partially adhered solutions was derived under the assumption that the adhesion energy is small,  $w_{ad} \ll 1$ . Within this approximation we found that delaminated solutions are always energetically preferable over adhered solutions, given that the natural curvature of the shell,  $\kappa$ , is made large enough compared to  $w_{ad}$ . To facilitate comparison with experiments, the delamination criteria that we found in Sec. IV B are summarized in Table I and compared with the expected behavior on a rigid substrate. Although the predictions of our theory have not been tested experimentally, we can yet compare our delamination criteria with the experiments reported in Ref. [37]. In the latter experiments narrow strips of spherical shells were deposited on a water substrate. Considering the typical parameters of the shells, i.e., thickness  $30 \mu\text{m}$ , Young's modulus  $1.5 \text{ MPa}$ , radius of curvature  $4\text{--}15 \text{ cm}$  and  $L/l_w \gg 1$ , the softness of the substrate,  $K = 10^4 \text{ N/m}^3$ , and the surface tension  $w_{ad} \simeq 0.1 \text{ N/m}$ , we find that the critical radius of curvature for delamination is  $\kappa_{cr}^{-1} \sim 10^{-2} \text{ cm}$ , much smaller than considered experimentally. Indeed, delamination was not observed in the latter experiments. Alternatively, changing the thickness in the latter experiments to  $\sim 10^{-3} \text{ m}$ , and keeping the other parameters fixed gives  $\kappa_{cr}^{-1} \sim 3 \text{ cm}$ , much closer to the range of the prescribed natural curvatures.

We add several comments regarding the analysis. First, although we did not mention it explicitly, the total length of the shell,  $2L$ , must always remain much larger than the shell's thickness. Otherwise, our reduced dimensional elastic theory does not hold [39]. The thickness of the shell,  $t$ , enters the formulation through the bending modulus  $B \propto t^3$  and

TABLE I. Summary of main results in dimensional form.

Delamination criteria on soft and rigid substrates					
		$\kappa_{cr}$		$\ell_{cr}$	
Soft	$L < \ell_* = 2.77\ell_w$	$\sim 3\sqrt{2}\frac{\ell_c}{L^2}$	[Eq. (24)]	$L$	
Substrate	$L > \ell_* = 2.77\ell_w$	$\sim \frac{\sqrt{2}}{\ell_{ec}}(1 - 0.06\frac{\ell_w}{L})$	[Eq. (26a)]	$\sim (\frac{\pi}{\sqrt{2}} + 0.26\frac{\ell_w}{L})\ell_w$	[Eq. (26b)]
Rigid substrate	all $L$	$\frac{\sqrt{2}}{\ell_{ec}}$	[Eq. (11)]	0	

therefore affects the wrinkling length scale,  $\ell_w = (B/K)^{1/4} \propto t^{3/4}$ .

Second, the validity of Winkler's model and its ability to approximate the complex deformation of an actual elastic substrate has been discussed by several authors; see, for example, recent review on the subject in Ref. [48], or the discussion in Ref. [49]. In regard to our system, this approximation has the obvious limitation that lateral deformations (shear) are not taken into account in the calculations. This underlying assumption of the model remains plausible as long as the substrate is incompressible [3] and its deformation remains small compared with its stress-free configuration. Indeed, both of our approximated solutions in Secs. III and IV A complied with this smallness requirement. While in the case of partially adhered shells we assume that the normalized height at the point of delamination remains small,  $h(\ell/2) \propto w_{ad}^{1/2} \ll 1$ , in the case of completely adhered shells we assume that the normalized natural curvature remains small  $\kappa \ll 1$ . Any extension of this theory into regions that accounts for large deformations of the substrate must take under consideration nonlinear effects in the substrate's response. These nonlinearities can either be derived systematically as is considered, for example, in Ref. [66], or can assume a phenomenological description that extends the validity of Winkler's model [8,67].

Third, problems involving contact between two cylindrical rings, without the support of an adhesive foundation, had been previously considered, either when the two rings are elastically deformable [68] or when only one ring is deformable and the other is rigid [69]. Note that due to the periodic boundary conditions prescribed on these objects [70], the minimizing configurations are always independent on the spontaneous curvature,  $\kappa$ . Differently, in our analysis the elastic configuration has a free edge at  $s = L$ , and therefore  $\kappa$  enters the formulation through the boundary condition, Eq. (9b). Considering the system in Ref. [68], one possible

extension that may include a nontrivial contribution of the spontaneous curvature could be when an open circular ring, i.e., with  $\kappa \neq 0$ , is encapsulating a longer closed ring. Under this setup, the boundary conditions on the outer, opened, ring will depend on its natural curvature. Furthermore, an even more intriguing scenario would be to investigate the latter setup, of an open ring that is encapsulating a closed ring, when the whole system is supported on a soft foundation. We assess that in this configuration, the adhered length between the outer ring and the substrate will affect the contact length between the two rings, at least in some range of the parameter space.

Fourth, in our model we neglected the energy of the meniscus. Indeed, as discussed in Refs. [14,46] this contribution is of a higher order if one considers an expansion in powers of  $w_{ad}$ . Fifth, note that the elastic theory of inextensible shells that undergo cylindrical deformation, i.e., with zero Gaussian curvature, is similar to that of fluid membranes. The adhesion of these membranes to an underlying substrate has been the subject of many recent studies [71–73]. In particular, the present formulation suggests new route to investigate the adhesion of closed cylindrical vesicles to soft substrates [74]. Last, it would be of great interest to extend the present framework into two-dimensional shells that encompass nonzero Gaussian curvature. For example, one can ask the following question: What are the delamination criteria of a spherical shell or wavylike patterns [75] that are adhered to soft foundations?

## ACKNOWLEDGMENTS

We thank Lior Atia for many useful discussions that motivated this work and to Haim Diamant for critical reading of the manuscript. This work was supported in part by the Pearlstone Center for Aeronautical Studies.

- [1] K. Kendall, *J. Phys. D: Appl. Phys.* **4**, 1186 (1971).
- [2] H. Mei, R. Huang, J. Y. Chung, C. M. Stafford, and H.-H. Yu, *Appl. Phys. Lett.* **90**, 151902 (2007).
- [3] H. Mei, C. M. Landis, and R. Huang, *Mech. Mater.* **43**, 627 (2011).
- [4] H.-H. Yu and J. W. Hutchinson, *Int. J. Fract. Mech.* **113**, 39 (2002).
- [5] E. Cerda and L. Mahadevan, *Phys. Rev. Lett.* **90**, 074302 (2003).
- [6] D. Vella, J. Bico, A. Boudaoud, B. Roman, and P. M. Reis, *Proc. Natl. Acad. Sci. USA* **106**, 10901 (2009).
- [7] H. Diamant and T. A. Witten, *Phys. Rev. Lett.* **107**, 164302 (2011).
- [8] B. Audoly, *Phys. Rev. E* **84**, 011605 (2011).
- [9] O. Oshri, F. Brau, and H. Diamant, *Phys. Rev. E* **91**, 052408 (2015).
- [10] O. Kruglova, F. Brau, D. Villers, and P. Damman, *Phys. Rev. Lett.* **107**, 164303 (2011).
- [11] F. Brau, *Phys. Rev. E* **90**, 062406 (2014).
- [12] F. Brau, P. Damman, H. Diamant, and T. A. Witten, *Soft Matter* **9**, 8177 (2013).
- [13] T. J. W. Wagner and D. Vella, *Phys. Rev. Lett.* **107**, 044301 (2011).
- [14] E. Hohlfield and B. Davidovitch, *Phys. Rev. E* **91**, 012407 (2015).

- [15] J. Hure, B. Roman, and J. Bico, *Phys. Rev. Lett.* **106**, 174301 (2011).
- [16] T. J. W. Wagner and D. Vella, *Soft Matter* **9**, 1025 (2013).
- [17] L. Pocivavsek, R. Dellsy, A. Kern, S. Johnson, B. Lin, K. Y. C. Lee, and E. Cerda, *Science* **320**, 912 (2008).
- [18] A. Epstein, D. Hong, P. Kim, and J. Aizenberg, *New J. Phys.* **15**, 095018 (2013).
- [19] O. Oshri and H. Diamant, *Phys. Chem. Chem. Phys.* **19**, 23817 (2017).
- [20] S. S. Velankar, V. Lai, and R. A. Vaia, *ACS Appl. Mater. Interfaces* **4**, 24 (2012).
- [21] A. Ghatak, L. Mahadevan, J. Y. Chung, M. K. Chaudhury, and V. Shenoy, *Proc. R. Soc. Lond. Ser. A* **460**, 2725 (2004).
- [22] A. Ghatak, L. Mahadevan, and M. K. Chaudhury, *Langmuir* **21**, 1277 (2005).
- [23] F. Brau, S. Thouvenel-Romans, O. Steinbock, S. S. S. Cardoso, and J. H. E. Cartwright, *Soft Matter* **15**, 803 (2019).
- [24] J. A. Rogers, T. Someya, and Y. Huang, *Science* **327**, 1603 (2010).
- [25] N. Lu and D.-H. Kim, *Soft Rob.* **1**, 53 (2014).
- [26] L. Pocivavsek, J. Pugar, R. O’Dea, S.-H. Ye, W. Wagner, E. Tzeng, S. Velankar, and E. Cerda, *Nat. Phys.* **14**, 948 (2018).
- [27] L. Pocivavsek, S.-H. Ye, J. Pugar, E. Tzeng, E. Cerda, S. Velankar, and W. R. Wagner, *Biomaterials* **192**, 226 (2019).
- [28] H. Diamant, *Nat. Phys.* **14**, 878 (2018).
- [29] N. Nguyen, N. Nath, L. Deseri, E. Tzeng, S. S. Velankar, and L. Pocivavsek, *Biomech. Model. Mechanobiol.* (2020).
- [30] A. J. O. Butler, C. R. Meyer, and J. A. Neufeld, *J. Appl. Mech.* **87**, 051010 (2020).
- [31] T. J. W. Wagner, T. D. James, T. Murray, and D. Vella, *Geophys. Res. Lett.* **43**, 232 (2016).
- [32] A. Libai and J. Simmonds, *The Nonlinear Theory of Elastic Shells* (Academic Press, New York, 1988).
- [33] Y. Zhou, C. M. Duque, C. D. Santangelo, and R. C. Hayward, *Adv. Funct. Mater.* **29**, 1905273 (2019).
- [34] S. Armon, E. Efrati, R. Kupferman, and E. Sharon, *Science* **333**, 1726 (2011).
- [35] R. M. Erb, J. S. Sander, R. Grisch, and A. R. Studart, *Nat. Commun.* **4**, 1712 (2013).
- [36] X. Yuan and Y. Wang, *Soft Matter* **16**, 1011 (2020).
- [37] O. Albarrán, D. V. Todorova, E. Katifori, and L. Goehring, [arXiv:1806.03718](https://arxiv.org/abs/1806.03718) [cond-mat.soft].
- [38] I. Tobasco, Y. Timounay, D. Todorova, G. C. Leggat, J. D. Paulsen, and E. Katifori, [arXiv:2004.02839](https://arxiv.org/abs/2004.02839) [cond-mat.soft].
- [39] L. D. Landau and E. M. Lifshitz, *Theory of Elasticity*, 2nd ed. (Butterworth-Heinemann, Oxford, 1986).
- [40] C. Majidi and G. G. Adams, *Mech. Res. Commun.* **37**, 214 (2010).
- [41] C. Majidi and G. G. Adams, *Proc. R. Soc. A* **465**, 2217 (2009).
- [42] C. Majidi, O. M. O’Reilly, and J. A. Williams, *Mech. Res. Commun.* **49**, 13 (2013).
- [43] G. Napoli and S. Turzi, *Proc. R. Soc. Lond. A* **471**, 20150444 (2015).
- [44] C. Majidi and K.-t. Wan, *J. Appl. Mech.* **77**, 041013 (2010).
- [45] B. Roman and J. Bico, *J. Phys.: Condens. Matter* **22**, 493101 (2010).
- [46] O. Oshri, Y. Liu, J. Aizenberg, and A. C. Balazs, *Phys. Rev. E* **97**, 062803 (2018).
- [47] S. T. Milner, J. F. Joanny, and P. Pincus, *Europhys. Lett.* **9**, 495 (1989).
- [48] D. A. Dillard, B. Mukherjee, P. Karnal, R. C. Batra, and J. Frechette, *Soft Matter* **14**, 3669 (2018).
- [49] M. A. Biot, *J. Appl. Mech.* **4**, 1 (1937).
- [50] Alternatively, we could as well normalize all lengths by the total length of the shell,  $L$ . Nonetheless, since the results of our analysis will depend strongly on this length scale, we prefer to keep it explicit in our formulation.
- [51] Note that, in general, another two Lagrange multipliers must be prescribed to account for the geometric constraints in the horizontal direction, i.e.,  $p_x^i(s)(\cos \phi_i - \frac{dx_i}{ds})$ . Nonetheless, we have omitted these terms in our formulation because there are no external forces acting on the system in  $x$  direction. Had we included these multipliers, we would have obtained after minimization that  $p_x^i(s) = 0$ .
- [52] H. Diamant and T. A. Witten, *Phys. Rev. E* **88**, 012401 (2013).
- [53] J. W. Hutchinson and Z. Suo, *Adv. Appl. Mech.* **29**, 63 (1991).
- [54] Z.-H. J. C. T. Sun, *Fracture Mechanics* (Elsevier, Amsterdam, 2012).
- [55] G. Gioia and M. Ortiz, *Delamination of Compressed Thin Films*, edited by J. W. Hutchinson and T. Y. Wu, *Adv. Appl. Mech.*, Vol. 33 (Elsevier, Amsterdam, 1997), pp. 119–192.
- [56] Had we replaced Eq. (10) with  $h_a(\ell) = 0$ , our set of equilibrium equations, Eqs. (5)–(10), would yield the trivial solution  $\ell = 0$ , i.e., completely detached cylinder.
- [57] H.-Y. Kim and L. Mahadevan, *J. Fluid Mech.* **548**, 141 (2006).
- [58] Note that in the derivation of  $\varphi_d$  we used the approximation  $w_{ad} \ll 1$ .
- [59] This is the first solution of the equation  $\tan(2q\ell) = \tanh(2q\ell)$ .
- [60] G. Napoli and S. Turzi, *Meccanica* **52**, 3481 (2017).
- [61] The contribution of the free edge is trivial, i.e., its shape is a circular arc with radius of curvature  $\kappa$ . Therefore, the energy of the free edge always vanishes, and it only provides a boundary condition to the inner, adhered, region.
- [62] D. A. Dillard, *J. Adhesion* **26**, 59 (1988).
- [63] B. Davidovitch and V. Démery, [arXiv:2007.04748](https://arxiv.org/abs/2007.04748) [cond-mat.soft].
- [64] Numerical investigation indicates that the size of this barrier is  $\Delta E_{bar} \simeq 0.1\ell_w/B$ .
- [65] Note that since the delaminated solution is physically accessible only when  $L > \ell$  (see discussion at the end of Sec. III), the adhered-to-delaminated transition will only occur when  $\kappa > \kappa_{cr} + \epsilon$ , where  $\epsilon$  is arbitrarily small.
- [66] F. Brau, H. Vandeparre, A. Sabbah, C. Poulard, A. Boudaoud, and P. Damman, *Nat. Phys.* **7**, 56 (2011).
- [67] T. C. T. Michaels, R. Kusters, A. J. Dear, C. Storm, J. C. Weaver, and L. Mahadevan, [arXiv:1906.04638](https://arxiv.org/abs/1906.04638) [cond-mat.soft].
- [68] G. Napoli and A. Goriely, *Proc. R. Soc. A* **473**, 20170340 (2017).
- [69] R. De Pascalis, G. Napoli, and S. Turzi, *Physica D* **283**, 1 (2014).
- [70] E. Katifori, S. Alben, and D. R. Nelson, *Phys. Rev. E* **79**, 056604 (2009).
- [71] M. Tanaka and E. Sackmann, *Nature* **437**, 656 (2005).
- [72] E. T. Castellana and P. S. Cremer, *Surf. Sci. Rep.* **61**, 429 (2006).
- [73] H. Noguchi, *Soft Matter* **15**, 8741 (2019).
- [74] U. Seifert, *Phys. Rev. A* **43**, 6803 (1991).
- [75] Y. Klein, S. Venkataramani, and E. Sharon, *Phys. Rev. Lett.* **106**, 118303 (2011).